Nucleation of product phase in reactive diffusion of Al/Co

V. Vovk, G. Schmitz,* and R. Kirchheim
Institut für Materialphysik and SFB 602, Georg-August-Universität, Hospitalstrasse 3-7, 37073 Göttingen, Germany
(Received 4 June 2003; revised manuscript received 7 October 2003; published 15 March 2004)

The reactive interdiffusion of Co/Al bilayers is studied by atom probe tomography. For that, metallic thin films were deposited on tungsten substrates preshaped by field evaporation. Owing to the outstanding resolution of the method and its real three-dimensional analysis, the nucleation of the first product could be characterized in detail. It is clearly seen that interdiffusion of the initial Al and Co layers precedes the formation of the first nuclei. A critical gradient for the onset of nucleation is determined to be 0.3 nm^{-1}. The Al_9Co_2 phase is identified as the first reaction product by direct chemical analysis. Instead of a layer, this phase forms as globular nuclei, which quickly grow to a thickness of about 10 nm before a dense layer has developed. The observed growth is understood by fast transport along incoherent interphase boundaries. For this condition, a kinetic model is discussed that describes the growth of the particles. The thickness at impingement is controlled by the ratio of the transport coefficients along and across the boundary. Choosing realistic values for the latter parameters, noninteger growth exponents ranging from 2 to 3 are predicted. Thus, the reaction proceeds much faster than in the case of ordinary parabolic or linear growth. After consumption of pure Al, the formation of B2-ordered AlCo is observed as the second stage of reaction.

DOI: 10.1103/PhysRevB.69.104102 PACS number(s): 64.70.Nd, 66.30.Pa, 68.37.Vj, 68.55.Ac

I. INTRODUCTION

Technological progress is managing its pace towards nanoapplications. On a continuously decreasing length scale different materials are packed together to build functional compounds. Under this condition, the stability of or the reaction at, the related interfaces often gets an important issue for the desired application. With further miniaturization earliest reaction stages, when the size of potential reaction products reaches only a few nanometers, attract particular attention.

The study of so-called thin-film reactions got popular already in the early time of microelectronics, when silicides have been used to form suitable contacts for the first time. Soon it was noticed that the physical understanding of bulk interdiffusion couples, which are defined by concurrent parabolic growth of all the expected equilibrium phases, is not sufficient in the case of thin films, or more general in the early stages of the reaction. Usually, only one product phase forms at the beginning, sometimes even a metastable one, as in the most prominent example of solid-state amorphization. Even after several decades of research a general model for this phase selection is still unavailable. Empirical rules have been developed with increasing success[1,2] but they still await a sounded justification.

The suppression of the lacking phases may be understood by the different volume diffusivities among the intermetallics under consideration. Since the diffusion coefficients vary by several orders of magnitude, a phase of low diffusivity may be expected in the steady state of transport with a theoretical thickness below 1 Å making the phase practically nonexistent.[3] As an alternative, kinetic barriers at the layer interfaces have been made responsible for the suppression of phases. Since the interfacial transport coefficients are usually unknown, the predictive power of this concept is rather low. Furthermore, linear growth regimes, which are a prerequisite for the validity of the model, have not been clearly proven yet for metallic reaction couples.

All the mentioned models take the nucleation of the product phase for granted, which has been usually justified by the enormous thermodynamic driving forces of the reaction, so that the size of a nucleus ranges down to below 1 nm. However in the last decade, indications got increasingly obvious that nucleation is nevertheless an important, rate determining step during the reaction of metals. This evidence stems mainly from scanning calorimetry, where the reaction to a unique product phase is reflected by two distinct exothermic peaks. Such a behavior is remarkably often observed with Al as a reacting component, e.g., Al/Nb, Al/Ti,[4], Al/Ag,[5] and Al/Co,[6] and is usually interpreted as a two-stage mechanism separating nucleation inside the interface from the thickness growth after forming a dense layer.[7]

Our study especially concentrates on the nucleation of the first product. Up to now details of this process are rather unclear. To which extent is mixing of the components an important prerequisite for nucleation? A real nucleation theory formulated in analogy to the cluster kinetic models of decomposition is still lacking. The difficulty in the description arises from the second reaction channel that always competes with the formation of the new product phase: the mere interdiffusion of the initial phases. Thus, the matrix, in which the potential nuclei are embedded, varies in time. As a consequence, a nucleus of the product phase, overcritical with respect to its surroundings at given time, will find itself undercritical to a later moment, which may result in a nonmonotonous evolution of the reaction. A first attempt to describe this complex situation quantitatively was undertaken recently by Gusak.[8]

In order to understand an eventual nucleation barrier, the influence of the composition gradient at the interface had been considered theoretically. It was found that the strong variation of composition at the initial interface may elevate

the barrier, so that nucleation gets impossible as long as a certain critical gradient is exceeded. Several concepts for the calculation of this critical limit have been introduced,[9–11] which are based on different microscopical mechanisms, so that its correct value is still unclear yet. However, estimating the critical gradient with one or the other theoretical concept based on realistic material parameters, typically a value of one over a few nanometer is found. To investigate reactions on such a short-ranged length scale, advanced analysis methods of outstanding spatial resolution are required. In addition, one has to expect that local nucleation may lead to complex morphologies, which cannot be investigated by classical depth profiling techniques providing only one-dimensional (1D) information. Therefore, we applied in this study atom probe tomography, as this technique yields real 3D information with a spatial resolution of a few angstroms and furthermore single-atom sensitivity.

We chose Al/Co as a model system, since for this binary reaction couple rather clear differential scanning calorimetry (DSC) measurements have been published and interpreted in terms of a two-stage nucleation and growth model.[6] Furthermore classical x-ray diffractometry indicates that the equilibrium phase most rich in Al forms as the first product, which is naturally explained by the strong increase of the atomic mobility with increasing Al content. Insofar, it is expected that this particular reaction couple represents more or less a general trend, while, e.g., Ni/Al, of which the binary phase diagram is quite comparable, represents an exceptional case: At first the formation of an unexpected B2 phase in off-stoichiometric composition is reported, although this phase with its very high melting point and ordered structure is distinguished by a rather low mobility.

II. EXPERIMENTS

In order to study reactive diffusion by atom probe tomography, layer interfaces must be prepared into specimen tips of only 20–50 nm curvature radius. For that, Co/Al bilayers were deposited onto substrate tips. Electropolished tungsten tips were field developed inside a field ion microscope up to a dc voltage of 12 kV to achieve an optimum substrate shape. These tips were coated with a Co and Al layer, 20 and 50 nm in thickness using a sputter deposition chamber, which is described elsewhere.[12] Background pressure inside the sputter chamber was 1×10^{-5} Pa, and the growth rate about 3 nm/min at room temperature. A typical specimen is shown in Fig. 1. Under the chosen growth conditions, especially inside the Al layer a rather coarse-grain size develops, so that no grain boundary is observed in the analyzed volume. Inside Co, the grain size appears to be significantly smaller. Since Al and Co need very different evaporation fields, Al was always deposited on top of Co. This way, the tip voltage can be increased monotonously during the measurement to obtain stable evaporation conditions. To perform the atomic reconstruction after the measurement, the tip radius $R(t)$, increasing during the measurement, is inferred from a geometric construction that takes into account the initial radius and a constant shaft angle as described elsewhere.[13] The latter two parameters are adapted to calculate a realistic evaporation field strength from the tip voltage by

$$\beta E_{evap}=\frac{U_{tip}}{R(t)}.$$

A typical trace of βE_{evap} is depicted in Fig. 2 demonstrating the different evaporation fields related to the various phases. Analysis was performed at 25 K in a voltage range from 5 to 15 kV, a pulse to base voltage ratio of 20%, and a pulse rate of 2 kHz. A typical mass spectrum obtained from the thin-film specimens is presented in Fig. 3. Using a low evaporation temperature noise can be limited to an acceptable level. Beside hydrocarbide impurities (H, C, O) are identified. The overall concentration of these elements amounts to below a

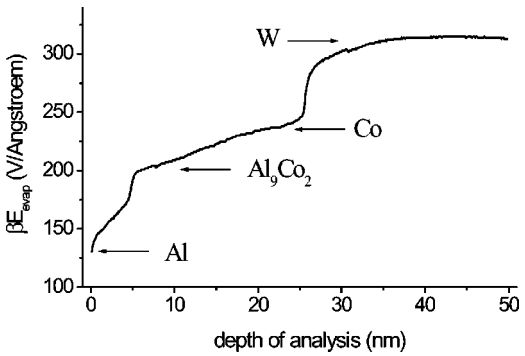

FIG. 2. Development of evaporation field strength during the analysis of a layered tip sample after a moderate heat treatment.

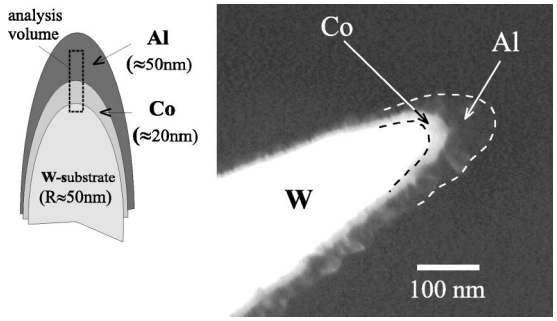

FIG. 1. Geometry of reaction couples used for atom probe tomography.

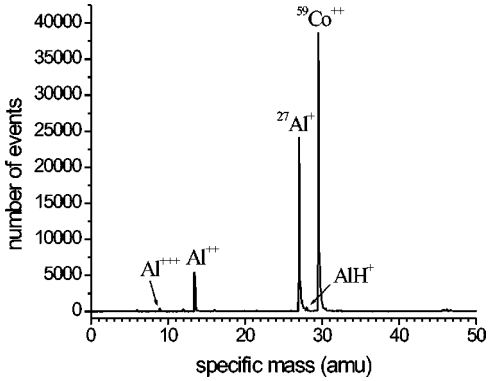

FIG. 3. Mass spectrum obtained by atom probe analysis of an Al/Co bilayer.

few pro mil. They are only observed at the beginning of measurement or at the transition between phases, when field conditions are not ideal, since the tip voltage must be adjusted to the new evaporation field as shown in Fig. 2. Thus we presume that the impurities are not contained inside the specimen, but stem from finite vacuum quality and specimen surface contamination. The important elements (Al, Co) are distinguished without any ambiguity by peak overlap. A general introduction to atom probe tomography may be found in Ref. 14.

To prepare different reaction stages, the coated tips were heat treated using an UHV furnace with a background pressure of 10^{-6} Pa. Since the annealing time is restricted for practical reasons to a range between 5 min and 1 h, the reaction could not be followed isothermally. Temperature had to be varied to observe early as well as late stages of the reaction.

III. RESULTS

In Fig. 4(a), the atomic reconstruction obtained at the interface of a specimen in the as-prepared state is shown. Since the curvature radius of the tips is significantly larger than the lateral width of the analyzed volume, the interface between the metallic layers appears to be almost planar. Inside the tungsten substrate individual (110) lattice planes are resolved. With their help the reconstruction is reliably scaled. The layerlike morphology is pertained in early annealing stages up to about 300 °C/5 min. However, the outstanding depth resolution of the atom probe allows to detect even minor modifications at the interface as is demonstrated by the 1D composition profiles in Fig. 4(b). These profiles have been determined normal to the interface. A certain degree of intermixing on the depth of about 1 nm is noticed already in the as-prepared state. Such a behavior is rather typical for sputtered multilayers of attractively interacting metals.[12,13] The zone of mixing broadens in the early stages up to 4 nm in thickness as shown in the inset of Fig. 4(b). But the shape of the profiles stays in reasonable agreement to an error function, suggesting a simple interdiffusion process.

By contrast, the formation of any new product phase should be indicated by a preferred composition or at least an unregular slope along the profiles. Such a ''fingerprint'' for the formation of a new phase is observed in some of the measurements after annealing to 300 °C/5 min. Globular regions that are distinguished by a more or less homogeneous composition close to that expected for the Al_9Co_2 equilibrium phase appear as shown in Fig. 5(a). These particles are found always on the Al side of the interface. They do not form a dense layer at the beginning, i.e., the layerlike reaction morphology is broken by local nucleation. The probable geometry derived as a summary of several atomic reconstructions is presented in Fig. 5(b). We assume in agreement with statements in recent literature[6] that triple joints between grain boundaries and the layer interface serve as heterogeneous nucleation sites. Since the lateral width of analysis is small compared to the grain size, the respective grain boundaries may lie well outside the reconstructed volume.

It is remarkable that the thickness of the freshly formed

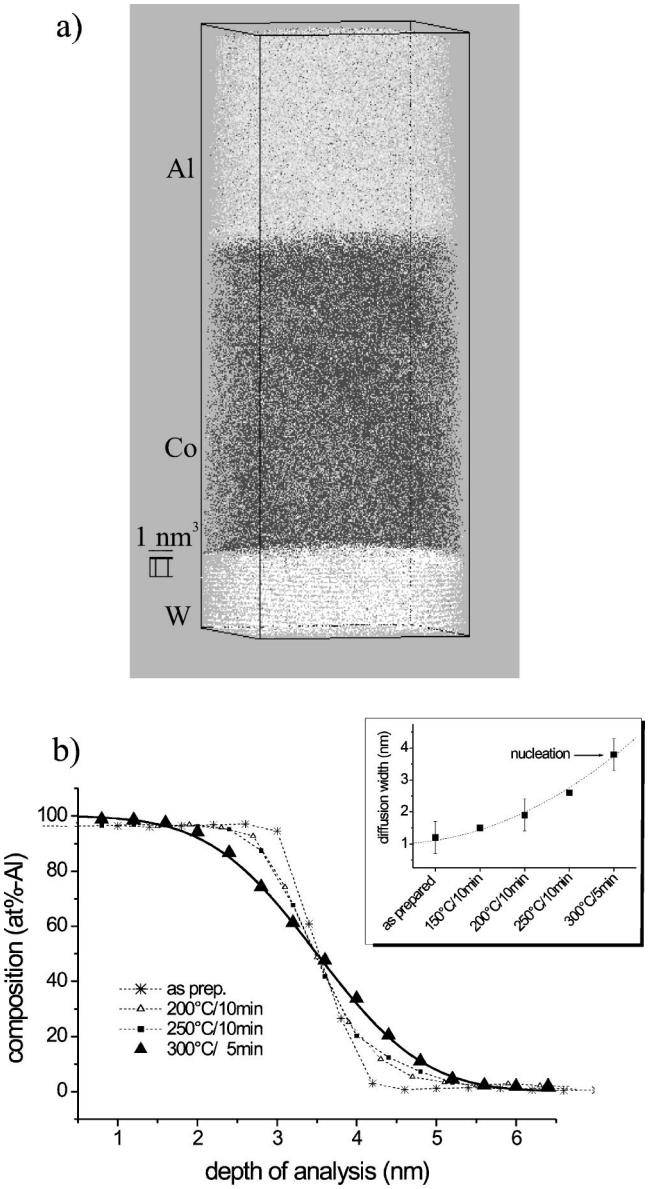

FIG. 4. (a) Atomic reconstruction of an Al/Co bilayer in the as-prepared state deposited on top of tungsten substrate tip. The positions of analyzed atoms are marked by color-coded dots. (b) Composition profiles determined normal to the Al/Co interface after heat treatments as indicated. The statistical error of each data point amounts to about ± 1 at.%. The solid line represents the error-function-like solution of thick-film interdiffusion. The increase of diffusion length between 5 and 95 at. % of the profiles is depicted in the inset.

particles is already considerably larger than the interdiffusion length observed after identical heat treatment at the original interface. This is demonstrated by the two composition profiles in Fig. 5: (c) through the initial interface beside the particle shown in Figs. 5(a) and 5(d) across a Al_9Co_2 particle. Obviously, the transport mechanism changes dramatically after a particle has nucleated, so that mixing gets much more efficient then.

Between specimens of identical annealing considerable statistical scattering is observed. Treatment at 300 °C for 5

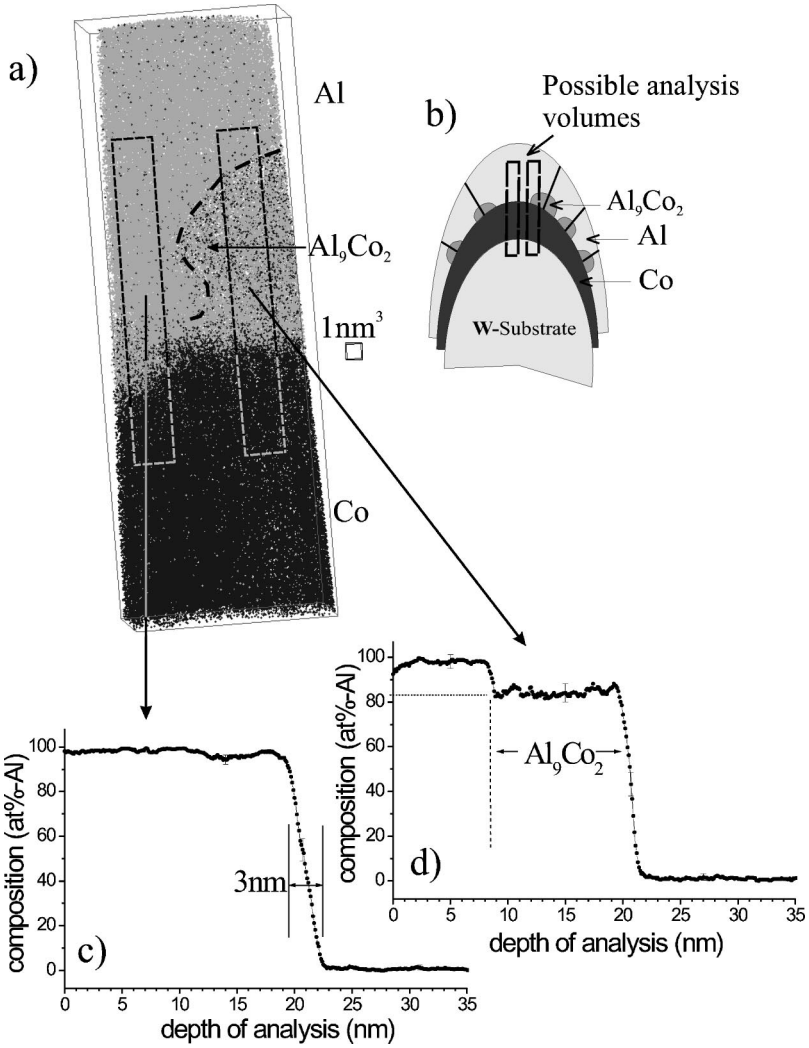

FIG. 5. Nucleation of first product phase. (a) Atomic reconstruction of a specimen after 5 min annealing at 300 °C; Co atoms, black dots; Al atoms, light gray dots. (b) Sketch of morphology. Composition profiles determined from the reconstruction: (c) through the Al/Co interface beside the particle (left side), (d) across the particle (right side) revealing the expected stoichiometric composition.

min reveals in some cases only interdiffusion at the interface, in other cases already a local particle of the product. After 10 min, we usually observe a closed Al_9Co_2 layer as a result of particle impingement. However, the thickness of this layer varies significantly as demonstrated by the concentration profiles in Fig. 6. These variations from measurement to measurement emphasize the statistical nature of the nucleation process taking place at this reaction stage. At even later stages, obviously after consumption of the remaining pure Al, a second product appears inside the reaction zone. This is proven by the distribution of cluster compositions. For that, the analyzed volume around the interface is divided into subvolumes of 50 atoms each. The frequency of these clusters as determined at a specimen after annealing at 450 °C for 10 min is plotted versus their composition in Fig. 7. Beside the peak of pure Co and that of the already discussed Al_9Co_2 phase, a further maximum evolved at about 50 at. %. Based on a comparison with the equilibrium phase diagram, this must be interpreted as the formation of the B2 ordered AlCo phase.

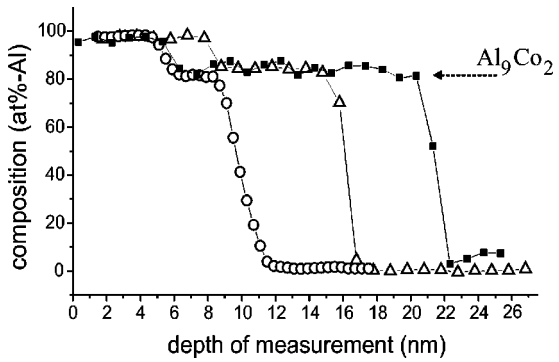

FIG. 6. Composition profiles determined across the dense Al_9Co_2 layer formed by annealing at 300 °C for 8 min (compact squares) and 10 min (open symbols). Thicknesses between about 3 nm and 15 nm are observed.

The atomic reconstruction of such a specimen after 5 min annealing at 450 °C is depicted in Fig. 8(a). In this case, already a dense layer of AlCo has formed. The related composition profile through this layer indicates an average composition of 43.8 ± 1 at. % Al, see Fig. 8(c). Thus, provided that the interpretation as B2 phase is correct, the composition lies almost exactly at the boundary of the phase field towards the Co side. It is remarkable that the composition profile reveals an absolutely flat composition plateau inside the

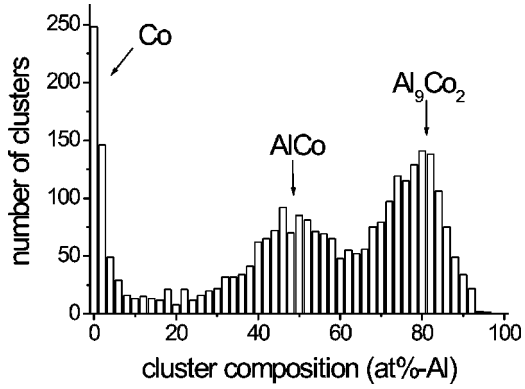

FIG. 7. Frequency distribution of clusters with 50 atoms each, vs composition as determined from the reaction zone after 5 min annealing at 450 °C.

phase region, while the phase diagram predicts an existence range of about 10 at. %. In the steady state of diffusion, one would expect the composition varying from the Al-rich side towards the Co-rich side of the existence range, in order to preserve the gradient driving force to further transport. Obviously, the growth of the second product follows other kinetic mechanisms.

Related to this, two other points are worth mentioning: (i) Evaluating various reconstructions in situations where the B2 phase still does not form a closed layer, it gets obvious that the AlCo phase always forms inside the Co layer; (ii) several reconstructions indicate the importance of grain boundaries inside the Co layer and so does the exemplary reconstruction in Fig. 8(a). Clearly the transport of Al and the formation of the new product proceeds along two-dimensional defects, which are reasonably interpreted as grain boundaries crossing the Co layer. In consequence, the likely geometry of the second reaction stage looks like that indicated in Fig. 8(b).

IV. DISCUSSION

The presented experimental results yield insight in the details of the early reactive diffusion on the nanometer length scale. In particular it is seen that nucleation is the rate limiting factor in the very beginning of the reaction so that interdiffusion of the initial components takes place in the mean time. Furthermore it is demonstrated that ordinary volume diffusion with a unique diffusion coefficient is not sufficient to describe the growth of the product phase. In the following, three aspects that seem to be important are further considered.

A. Suppression of nucleation by concentration gradients

Our experiments definitely prove that the formation of the first product phase is preceded by the mixing of the initial components. However, this mixing appears only on the tiny length scale of 3.5 nm. The mechanisms of nucleation at a reactive interface have been discussed in recent literature. Different scenarios may be distinguished termed as the (i) polymorphic mode,[9] i.e., the transformation into the new lattice structure without any compositional relaxation is the rate

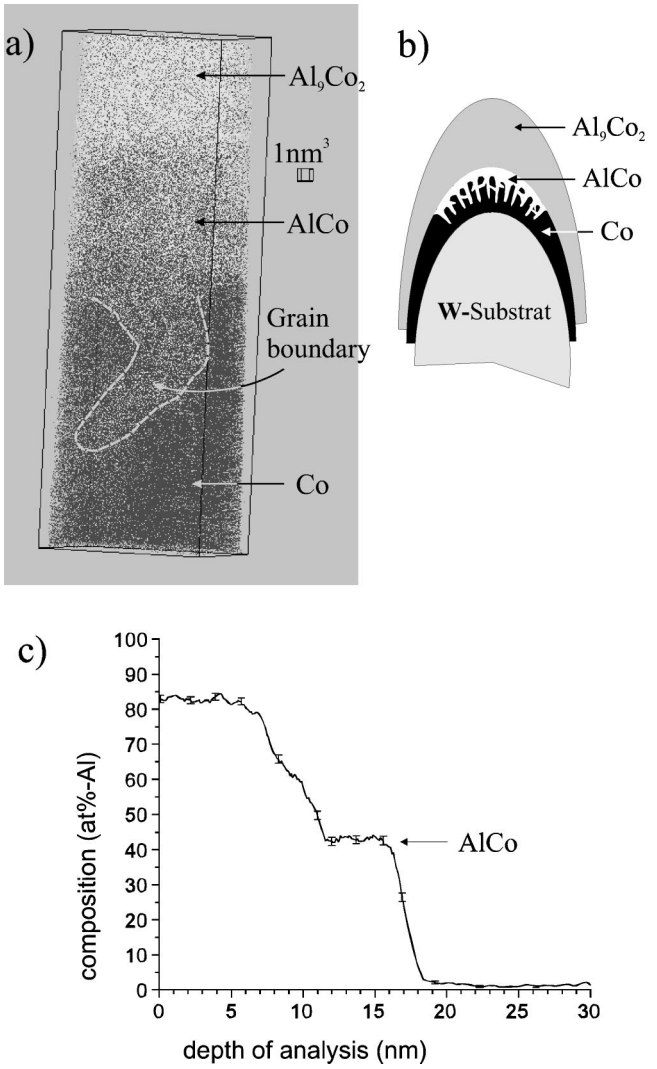

FIG. 8. (a) Atomic reconstruction of a specimen after 5 min annealing at 450 °C. The region of grain-boundary transport is marked by a dashed line. (b) Sketch of the reaction geometry. (c) Composition profile across an AlCo layer embedded between Al_9Co_2 and pure Co. Its composition is found homogeneously at (43.8 ± 1) at. % Al.

limiting step, (ii) the transversal mode, which allows the compositional relaxation between the new particle and the surrounding matrix by lateral diffusion,[10] and (iii) the complete mixing mode,[11] in which the nucleus is directly formed in its ideal stoichiometric composition. The nucleation barrier depends on the choice among these microscopic models. The first two models predict a certain critical composition gradient that must be established by diffusion before nucleation gets possible, while in the latter complete mixing mode nucleation is possible already at an absolutely sharp interface. In addition, a shape optimization of the nucleus must be considered, which leads to a further reduction of the barrier.[15] In a forthcoming paper,[16] we will present a comparison of the critical gradient determined by the atom probe analysis with different theoretical predictions. In the case of Co/Al, a quantitative agreement with the experimental data seems to be achievable only by the polymorphic mode in-

cluding the shape optimization of the early particles. Though transversal mode also predicts critical composition gradient for the beginning of nucleation, its value is too high in comparison with the experimental data presented in this paper.

B. Mechanism of atomic transport

In classical studies on thin-film interreactions often a parabolic or linear growth kinetics of the product phase is predicted and discussed. However, one has to realize that this prediction is an inevitable consequence of the assumed simple geometry given by a stack of homogeneous layers. Since the reaction is understood by one-dimensional diffusion, the transport of one or the other component across the product layer is required to drive the reaction. The situation dramatically changes, if the complex microstructure inside thin films is considered. Globular nuclei may grow into two or three dimensions. In this case, short cut diffusion along the surrounding matrix phase makes the transport through the product obsolete. In addition, grain and phase boundary diffusion may allow the fast transport along a complex network of two-dimensional surfaces.

Calorimetric studies of reactive diffusion with different combinations of metals demonstrated that the formation of the first product proceeds often via two well distinguished steps, of which nucleation of first particles and their lateral growth along the interface mark the initial reaction stage.[4] Compared to later growth in normal direction, the lateral spread along the interface is very fast, which is usually explained by the fact that for the formation of a first closed layer no long-range transport is required, since both components exist at the interface in abundance. However, by a quantitative evaluation of the heat releases, the thickness of the first layer is usually found at about 10 nm, in the case of Al/Ag even a thickness of 50 nm has been reported. This value significantly exceeds the critical size of a nucleus, which typically ranges down to 1 nm. Our microscopical observation confirms this interpretation of the DSC data since the observed globular particle and early layers are observed in a thickness ranging from about 5 to 15 nm. Obviously, already the formation of the first closed layer requires considerable atomic transport normal to the original interface, which makes it difficult to understand, why this diffusional process should proceed at much lower temperature than the later thickness growth.

However, the nanoanalysis indicates that this fast growth is not provided by ordinary volume diffusion. During the same annealing treatment volume diffusion in the parent phase leads to a mixing on only 3.5 nm depth, while some particles grow to even more than 10 nm in thickness. Probably, the volume diffusion coefficient of the complex intermetallic structure containing 22 atoms in the unit cell will be even less than that of the pure Al matrix. In consequence, material must be transported towards the particle via the phase boundary between Al_9Co_2 and the surrounding matrix as illustrated in Fig. 9. Due to the complex structure of the intermetallic, the boundary is very likely an incoherent one, which makes fast boundary transport a quite reasonable assumption.

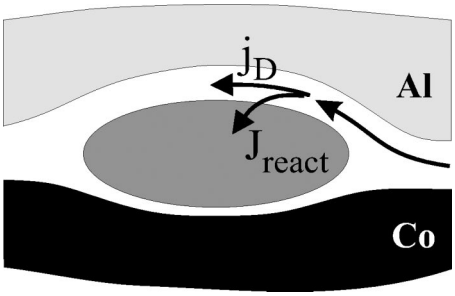

FIG. 9. Transport currents in the first growth state of the nuclei.

In addition, the observed asymmetric particle position at the Al side of the reaction couple indicates that only the interface towards the Al layer is active in this way, whereas the interface between the intermetallic and cobalt does not play an important role for the early particle growth. The heterogeneous transport has important consequences for the growth kinetics and the shape of the early particles as will be discussed in the following section.

A rather similar conclusion has to be drawn for the growth of the B2 AlCo phase. In this case, the transport along grain boundaries of the Co layer is directly proven by atomic reconstructions as that shown in Fig. 8(a). Besides, also indirect evidence confirms this interpretation. If the growth of the particle is driven by the transport through itself, a compositional variation from the Al to the Co side would have to be expected in a range of about 10 at. %, according to the phase diagram. By contrast, the experiments reveal a homogeneous composition. However, the constant composition is easily understood by transport towards the particles along the surrounding grain boundaries of the Co layer. This way, the particle gets embedded into a Co-rich alloy, which naturally explains that the composition of the intermetallic product is constant and agrees just to the Co-rich side of the phase existence range in the phase diagram.

C. Growth of early particles

In the following, the growth of an individual particle is considered with a rather simplified model that takes into account the interfacial transport. Nevertheless, it enables to understand the considerable thickness of the first closed layer, and furthermore it yields a quantitative prediction for the time exponent of the reaction kinetics in terms of the transformed volume fraction. Looking for the most simple but sufficient ansatz, we assume that volume diffusion is completely frozen. Also lattice mismatch, reaction induced stress, and energetic contributions of the interfaces are ignored. Our model is based on a recent suggestion by Lucenko and Gusak.[17] However, compared to their proposition, we use more appropriate boundary and growth conditions, which lead to a different particle shape and in consequence also to different time exponents.

The geometry underlying the description is shown in Fig. 10. A spherical nucleus is inserted at the interface. Opposed to the experimental observation, symmetric growth of the particle to both sides of the reaction couple is assumed to

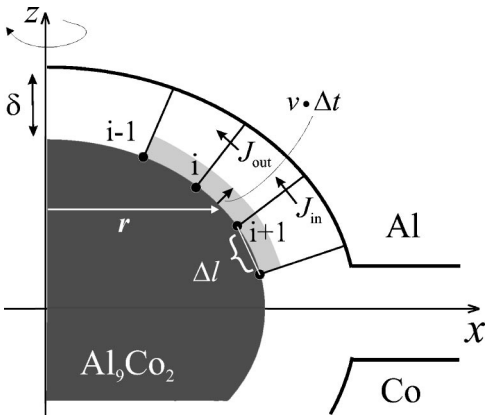

FIG. 10. Geometry to describe early growth of product particle.

allow the symmetrical formulation of boundary conditions. Compared to the real situation, this will just double the reaction rate and the exact shape at the triple junction to the interface may be predicted artificially. At the Al side, atoms of Co, being the minority component, diffuse from the initial interface into the interphase boundary Al/Al_9Co_2 to form an alloy with the Al atoms being present in abundance. If this alloy gets supersaturated, further growth of the particle is possible. The driving force to transport the minority component across the interface into the new particle stems from the difference between the actual chemical potential μ and that in equilibrium to the intermetallic μ_{eq}. Thus, we have for the migration velocity of the interface

$$v = -\frac{\Omega}{c_I} j = \frac{\Omega}{c_I} M(\mu - \mu_{\mathrm{eq}}) = \frac{1}{c_I} \frac{\Omega M k_B T}{c_{\mathrm{eq}}} (c - c_{\mathrm{eq}}) \quad (1)$$

$$\approx \frac{\kappa}{c_I} (c - c_{\mathrm{eq}}) \quad (2)$$

with Ω, c, c_I, j, M being atomic volume, atomic fraction of Co at the interface and in the intermetallic product, current density, and mobility of Co across the interface, respectively, and κ is an interfacial reaction constant, $\kappa = \Omega M k_B T / c_{\mathrm{eq}}$. Tacitly, deviations of the new intermetallic from equilibrium have been neglected.

Mass balance then predicts the development of the composition $c(l,t)$ inside the boundary to

$$\frac{\partial c(l,t)}{\partial t} = \frac{1}{r(l)} \; D_{\mathrm{PB}} \frac{\partial}{\partial l} \left(r(l) \frac{\partial c}{\partial l} \right) - \frac{v c_I}{\delta}. \quad (3)$$

The first term on the right-hand side describes ordinary diffusion along the interface with a boundary diffusion coefficient D_{PB}, while the second takes into account the loss of Co atoms into the growing particle. c_I is the stoichiometric composition of the product intermetallic and l a curvilinear coordinate defined along the particle surface with its origin at the axis of symmetry; further geometric variables are defined in Fig. 10. Together with suitable boundary conditions, Eqs. (2) and (3) are sufficient to describe the evolution of an isolated nucleus. Following the geometry of the problem, we postulate that the gradient of the composition profile must

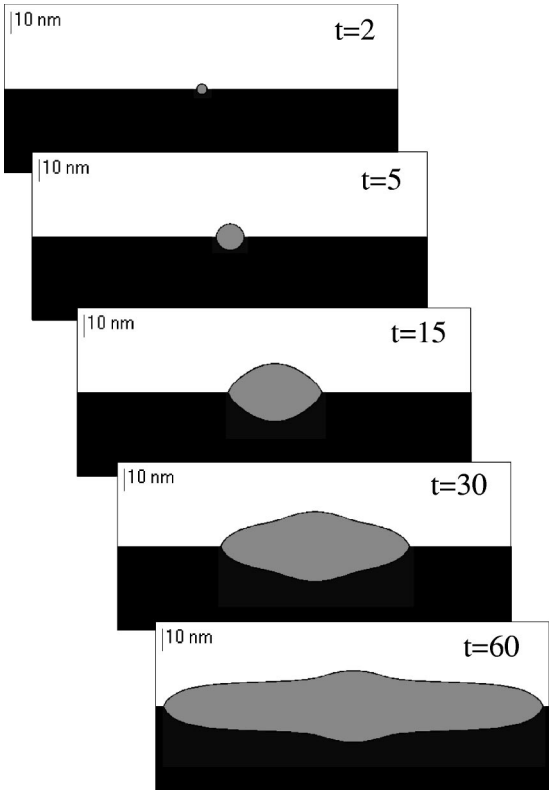

FIG. 11. Evolution of a spherical nucleus as calculated by Eqs. (2) and (3). Annealing time is stated in dimension-free, numerical units.

vanish at the axis of symmetry $\partial c / \partial l|_{l=0} = 0$. The interface between the initial reaction partners forms a reservoir of constant alloy composition, which is determined by the jump frequencies of Co and Al into the interface. Having no specific information, we just postulate an intermediate composition here, which yields as a second condition for the composition profile $c(l_{max}) = c_0 = 0.5$ at the outer rim of the particle.

To integrate Eq. (3) we start with a spherical nucleus. The initial profile $c(l)$ is defined at equidistant points along the perimeter with the composition linearly varying from $c|_{l=0} = c_{\mathrm{eq}}$ to $c|_{l_{\max}} = c_0$. The growth of the particle proceeds normal to its actual surface. With the growing particle the length of the perimeter increases so that further boundary points have to be inserted during the calculation to limit the truncation error. The quantitative prediction of the model depends on only two kinetic parameters, the interfacial diffusion coefficient D_{PB} and the reaction constant κ. A change of the ratio between them will modify the shape and thus the thickness of the first closed layer, while a proportional variation of both will only change the time scale of the reaction.

In Fig. 11 the development of a spherical product particle at the interface is shown as simulated by the integration of Eqs. (2) and (3) with a mobility ratio $\gamma := D_{\mathrm{PB}} / \kappa = 3 \times 10^{-8}$ m. It is clearly seen that the nucleus grows at first in a three-dimensional manner. But later normal growth ceases and the particle subsequently spreads along the interface in a two-dimensional mode. This behavior is naturally under-

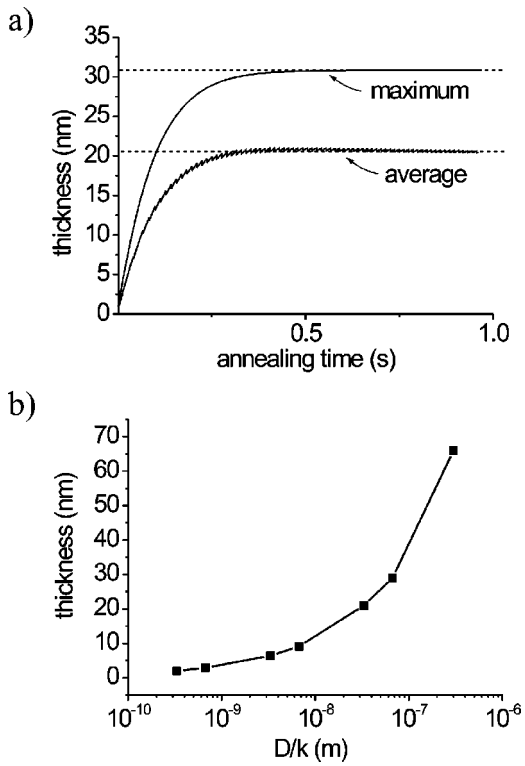

FIG. 12. (a) Thickness growth of the particle normal to the initial interface, measured at the axis of symmetry (maximum) or averaged over consumed area of the interface (average). (b) Dependence of the steady-state averaged thickness on the ratio $\gamma = D/\kappa$.

stood. Since at each position of the interface a portion of the Co current is consumed by the growing particle, the Co composition at the top and bottom area of the interface gets increasingly depleted with increasing diffusion length, so that these areas are prevented from further growth. This way, an asymptotic thickness of the product particle is established shortly after nucleation, as shown in Fig. 12(a). A reasonable boundary diffusion coefficient has to be chosen for a proper scaling of time in physical units. In the absence of profound data for CoAl, we estimate $D_{\mathrm{PB}} \approx 10^{-13}$ m^2/s adapted to grain-boundary diffusion data of Fe in Al.[18] The asymptotic thickness itself depends on the ratio $\gamma = D_{\mathrm{GB}}/\kappa$ as shown in Fig. 12(b). A comparison of this thickness with the experimental observation offers the possibility to estimate a numerical value for the reaction constant κ, which is difficult to determine otherwise, as in metals usually reactions are rate limited by diffusion. Keeping in mind the experimental scatter of the layer thickness and that in our symmetrical model the calculated thickness must be twice the experimental one, we estimate the appropriate ratio to $\gamma = 7\times10^{-9} - 7\times10^{-8}$ m and therefrom the reaction constant to $\kappa = 10^{-6} - 10^{-5}$ m/s. This reaction constant is that high that a linear growth regime will never be observed during reactive diffusion in agreement to the usual experimental situation with metals. The maximum thickness for linear growth estimated by

$$\Delta x = D_V/\kappa \tag{4}$$

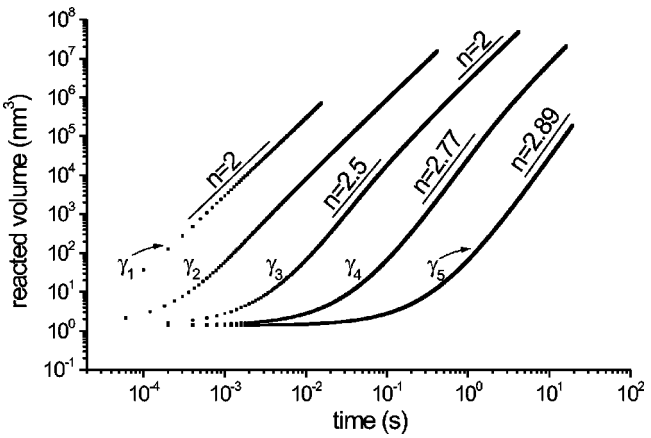

FIG. 13. Development of particle volume with time calculated for different mobility ratios: $\gamma_1 = 3.3\times10^{-10}$, $\gamma_2 = 3.3\times10^{-9}$, $\gamma_3 = 3.3\times10^{-8}$, $\gamma_4 = 3.3\times10^{-7}$, $\gamma_5 = 3.3\times10^{-6}$. The parameter n stands for the exponent in a power-law representation of the kinetics.

is smaller than 1 Å, when we compare κ with, e.g., the volume diffusion coefficient of Co in an Al matrix, which amounts to about 10^{-17} m^2/s at 300 °C.[19] At this thickness, neither the structure of the intermetallic with a lattice constant of at least 6.2 Å could be established nor a closed layer would have formed as demonstrated by the atom probe analysis.

The development of the particle volume is characteristic for the overall reaction kinetics as long as impingement does not happen. This volume is plotted versus time in the double-logarithmic representation of Fig. 13, calculated for different ratios of the mobility coefficients as stated in the figure. With small ratios (γ_1), i.e., a large reaction constant, all the Co at the interface immediately reacts to the intermetallic, so that growth proceeds in a two-dimensional manner, reflected by a kinetic exponent $n = 2$ almost from the beginning of the reaction. With increasing γ, i.e., lower reaction rate at the interface, the overall reaction slows down. For moderate particle sizes, Co is able to migrate even to the top of the particle resulting in almost three-dimensional growth, which is reflected by kinetic exponents close to 3. However, later when the particle has grown to a bigger size, thickness growth ceases and a transition of the kinetic exponent towards 2 is predicted. In the very beginning all the kinetic curves exhibit a kind of incubation behavior. As this is related to the initial composition profile along the interface of the early nucleus, the exact behavior at this stage is somewhat arbitrary.

The remarkable result of the presented rather simple model is the interesting feature that kinetic exponents significantly larger than 2 are possible, without any artificial assumption on the time dependence of the nucleation rate. Indeed, experimental data reveal in some cases rather high kinetic exponents, see the selected data collected in Table I. On the other hand, these data also demonstrate a large range of variation, which might be related to different microstructural situations. If the density of nucleation sites is rather high, impingement of the particles happens very early so that

TABLE I. Experimentally determined kinetic exponents.

Compound	Multilayer periodicity (nm)	Exponent	Technique
Al_3Ti	10	1.3	DSC (Ref. 4)
Al_3Ni	10	3.8	Isothermal DSC (Ref. 20)
Al_3Ni	20	2.5	Isothermal DSC (Ref. 20)
Ag_2Al	60	2.5	X-ray diffraction (Ref. 21)

according to the traces in Fig. 13 small exponents are dominant. In the opposite case of a low density of nucleation sites, each nucleus may grow into the square or cubic time regime in dependence on the ratio of interfacial diffusion coefficient and reaction constant, reflected by rather large kinetic exponents.

V. CONCLUSIONS

The earliest stages of reactive diffusion of Co/Al thin-film reaction couples have been investigated by three-dimensional atom probe analysis. Due to the outstanding resolution of this method, it could be demonstrated that the nucleation of the first product phase is preceded by the mere interdiffusion of both components. This diffusion appears on a maximum depth of 3.5 nm. Thus, a critical composition gradient for nucleation is determined to 0.3 nm^{-1}.

Nucleation of the first product Al_9Co_2 is observed after heat treatments at 300 °C for 5 min. The phase appears as globular particles, which quickly form a dense layer by particle impingement. As the second reaction product, an off-stoichiometric, Co-enriched AlCo phase is determined.

The local analysis clearly indicates the dominance of heterogeneous transport along the particle interfaces in the case of Al_9Co_2 and along the grain boundaries of the Co layer in the case of the formation of AlCo. Taking this heterogeneous transport into account, the growth of the early particles is modeled. The heterogeneous transport is shown to potentially result in three-dimensional particle growth and thus, in unexpectedly large time exponents in the range of 2–3.

ACKNOWLEDGMENTS

The authors are grateful to A. Gusak and his co-workers at Cherkassy State University for very valuable discussions and propositions. The support of the VW-foundation and the DFG that allowed the construction and maintenance of the tomographic atom probe is gratefully acknowledged.

*Present address: Institut für Materialphysik, Westfälische Wilhems-Universität Münster, Wilhelm-Klemm-Str. 10, 48149 Münster, Germany. Electronic address: gschmitz@nwz.uni-muenster.de; URL: http://www.uni-muenster.de/Physik/MP/gschmitz/schmitz.html

[1] R.M. Walser and R.W. Bené, Appl. Phys. Lett. **28**, 624 (1976).
[2] R. Pretorius, A.M. Vredenberg, and R.d.R.F.W. Saris, J. Appl. Phys. **70**, 3636 (1991).
[3] A.M. Gusak and K.P. Gurov, Phys. Met. Metallogr. **53**, 6 (1982).
[4] C. Michaelsen, K. Barmak, and T.P. Weihs, J. Phys. D **30**, 3167 (1997).
[5] R. Roy and S.K. Sen, J. Mater. Sci. **27**, 6098 (1992).
[6] C. Bergmann, E. Emeric, G. Clugnet, and P. Gas, Defect Diffus. Forum **194-199**, 1533 (2001).
[7] K.R. Coffey, L.A. Clevenger, K. Barmak, D.A. Rudman, and C.V. Thomson, Appl. Phys. Lett. **55**, 852 (1989).
[8] A.M. Gusak, F. Hodaj, and A.O. Bogatyrev, J. Phys.: Condens. Matter **13**, 2767 (2001).
[9] A.M. Gusak, Ukr. Phys. J. **35**, 725 (1990).
[10] P.J. Desré and R. Yavari, Phys. Rev. Lett. **64**, 1533 (1990).
[11] F. Hodaj and P.J. Desré, Acta Mater. **44**, 4485 (1996).
[12] J. Schleiwies and G. Schmitz, Mater. Sci. Eng., A **327**, 94 (2002).
[13] T. Jeske and G. Schmitz, Mater. Sci. Eng., A **327**, 101 (2002).
[14] T. Al-Kassab, H. Wollenberger, G. Schmitz, and R. Kirchheim, in *High-Resolution Imaging and Spectrometry of Materials*, edited by F. Ernst and M. Rühle (Springer, Berlin, 2003).
[15] F. Hodaj, A.M. Gusak, and P.J. Desré, Philos. Mag. A **77**, 1471 (1998).
[16] M. Pasichnyy, A. Gusak, V. Vovk, and G. Schmitz (unpublished).
[17] G. Lucenko and A. Gusak, *Proceedings of DIFTRANS'2001*, *Bulletin of Cherkassy State University*, Physics **34**, 1145 (2001).
[18] I. Kaur, W. Gust, and L. Kozma, *Handbook of Grain and Interphase Boundary Diffusion Data* (Ziegler Press, Stuttgart, 1989).
[19] A.D. LeClaire and G. Neumann, in *Diffusion in Solid Metals and Alloys*, edited by H. Mehrer, Landolt-Börnstein, New Series, Group III, Vol. 26 (Springer, Berlin, 1990).
[20] C. Michaelsen, G. Lucadamo, and K. Barmak, J. Appl. Phys. **80**, 6689 (1996).
[21] G. Schmitz, O. Svenson, P. Troche, and F. Harbsmeier, *Solid-Solid Phase Transformations JIM* (Japan Institute of Metals, Kyoto, 1999), p. 1283.